A Study of Surface Defects in Tb Doped ZnO Nanoparticles for Gas Sensing Applications

A. Sharma[1,a)] and V. N. Rai[2, b)]

[1]*Department of Sciences and Humanities, Room no. A017, Aryabhatt Building, K. J. Somaiya College of Engineering, Vidyavihar (E), Mumbai-400077*
2School of Physics, Devi AhilyaVishwavidyalay, Takshashila campus, Khandwa Road, Indore, M.P-452001

[1a)]Corresponding author: sharma.archana3@gmail.com, archana.sharma@somaiya.edu
2b)vnrai999@gmail.com

Abstract. New goals for providing better solutions with the help of nanotechnology have emerged from the electronics industry. Nano-electronics has focused on the structural, optical, magnetic, and photoluminescence properties of nanomaterials for developing optoelectronic devices. These properties play a vital role at the nanoscale level in comparison to that of bulk compounds. The use of semiconductor materials has always been in demand. Here, we are focusing on the unique and distinct structural and optical properties of rare earth-doped ZnO nanostructures. Nanoparticles of ZnO doped with Terbium ion was prepared by sol gel method. Systematic structural studies on Tb^{3+} ion doped ZnO nanocrystals were carried out using X-ray diffraction, High resolution transmission electron microscopy, X-ray photoelectron spectroscopy and EPR study. X-Ray photoelectron spectroscopy and EPR studies spectroscopy measurements were also performed on these nanoparticles to observe the surface property alteration done by rare earth incorporation. It was observed that by incorporation of Tb^{3+} ions, the broad band luminescence has enhanced which could be exploited for the fabrication of display devices of required luminescence. The EPR study shows that the type of surface defects changes for different concentration of Tb doped in the ZnO nanoparticles.

INTRODUCTION

Zinc oxide (ZnO) nanoparticles are found to have wide application in the field of display devices, LED's, gas sensors due to its remarkable properties like high electron mobility, wide band gap, eco-friendly nature, good thermal and chemical stability. The properties of ZnO have been extensively studied using various techniques like Electron paramagnetic resonance, Photoluminescence, photon correlation spectroscopy and many others[1,2]. In spite of the studies done on ZnO nanostructures, there are still many issues that are left unresolved like the presence of shallow donors or the origin of visible emission. Gas sensing behaviour of ZnO basically depends upon the interaction between the oxygen species (such as hydroxyl groups, acetate groups) that are adsorbed on the surface and the target gas molecules. Therefore, it becomes extremely important to understand the interaction between host oxide surface and target gas molecules for improving gas sensing performance of semiconductor metal oxides. Metal oxides such as ZnO, SnO_2, TiO_2 etc. exhibit good sensitivity but lack selectivity towards target gases. Many research groups have developed semiconductor metal oxide sensors by adding various elements as dopants [3, 4]. Electronic, chemical and surface properties of the host lattice can be altered by the substitution of an appropriate dopant element [5-7]. Rare earth elements are on high demands now a day for being used as dopants for various applications due to their highly magnetic, electrochemical and luminescent properties. Furthermore, for gas sensing applications, rare earth element doped metal oxides have proved to be promising candidates for improving sensing behavior because of their effective catalytic nature, fast oxygen ion mobility and high surface basicity [8, 9]. In this work we have used terbium rare earths as a dopant, because it generates defect which are associated with oxygen vacancies [8, 9]. Thus, it is expected to enhance the sensing performance as the level of non-stoichiometry of the host ZnO lattice increases due to oxygen vacancies induced through this rare earth dopant ion. In the present work, ZnO and Tb doped ZnO has been prepared by following wet chemical route. Here, we present a systematic study of the structural, morphological, elemental and optical properties of the synthesized ZnO and Tb doped ZnO nanoparticle samples. Our study suggests that the Tb incorporate mostly on the surface rather than in the core of the

ZnO nanoparticles. It has been found that the accumulation of Tb on the surface of the nanoparticles results in an enhancement in the surface defects as the ZnO lattice gets modified.

EXPERIMENTAL

Tb doped ZnO nanoparticles were synthesized by a sol-gel technique [10]. The structural properties of the nanoparticles were investigated by high resolution transmission electron microscopy (HRTEM) and X-ray diffraction (XRD), XPS and EPR studies. Optical properties were investigated through steady state photoluminescence (PL) and Absorption spectroscopy.

RESULTS AND DISCUSSION

The X-ray diffraction data and PL spectroscopy of the undoped and Tb doped ZnO nanoparticles has been reported elsewhere [10]. All the nanoparticle samples exhibited some emission spectrum in the visible spectrum. In order to observe the presence of paramagnetic defects, Electron paramagnetic resonance experiment was performed at room temperature at X- band frequency (9.5 GHz). Figure 1 compares the EPR spectra recorded for an undoped and a Tb doped ZnO nanoparticle sample with Tb mole fraction of x= 0.04.

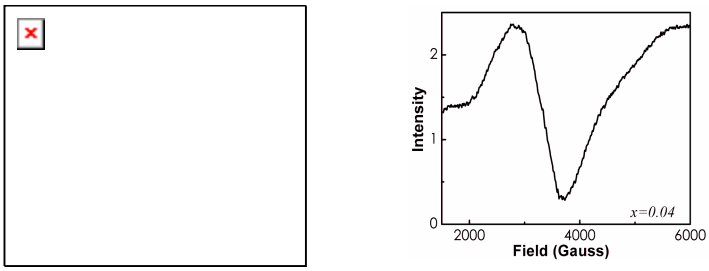

FIGURE 1: EPR spectra for an undoped ZnO nanoparticles and a Tb doped ZnO nanoparticles with Tb mole-fraction x = 0.04.

The value of g-factor of the samples was calculated using the equation $g = \Delta E / \mu_B B$. The estimated value of g-factor for ZnO nanoparticles comes out to be 2.13 while for the Tb doped ZnO nanoparticles with x=0.04, the g-factor value is 2.03. The obtained values are in good agreement with the values reported for chemisorbed oxygen species on the surface of these nanoparticles [11-13]. Chemisorbed oxygen species was reported to show a broad feature having g-value in the range of 2.007-2.05, which is in agreement with broad peak observed for our ZnO nanoparticle samples at room temperature. Therefore, we can conclude that the broad feature observed is due to adsorbed chemical species containing oxygen that are residing on the surface of the nanoparticle.

Figure 2 compares the survey scans for an undoped ZnO and a Tb doped ZnO nanoparticle sample (with Tb-acetate/Zn-acetate ~25%).

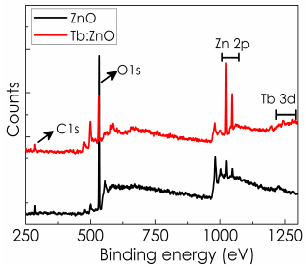

FIGURE 2. Survey scan for an undoped and a Tb doped ZnO nanoparticles for Tb-acetate/Zn-acetate ~ 25%).

In both the scans, the peaks associated with Zn, O and C are clearly visible. In Tb doped ZnO nanoparticles, Tb related features could be seen.

Figure 3 (a) and (b) shows the Gaussian deconvolutions of the XPS spectra for the O1*s* core level line of ZnO and a Tb doped ZnO nanoparticle sample (with Tb-acetate/Zn-acetate ~ 25%). In the XPS spectra, the open circles denote the experimental data, red solid line represents the fitting curves and the deconvoluted individual peaks are depicted with dashed green lines.

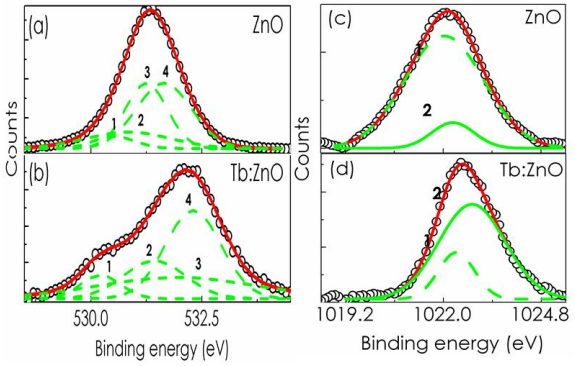

FIGURE 3.O1*s* XPS spectra (a, b) and Zn2$p_{3/2}$ (c, d) XPS spectra for ZnO and Tb doped ZnO nanoparticles for Tb-acetate/Zn-acetate ~ 25%. The open symbols in the figure represent the experimental data, thick solid (red curve) line represents the fitted data and thin solid lines (green curve) represent the components used to deconvolute the experimental peak.

The deconvolution of O1*s* peak shows the existence of four different oxygen species in the ZnO nanoparticles [Fig. 3(a)]. The peak centered at 530.52 eV (1) is reported to be associated with the Zn-O-Zn bonding in the wurtzite phase of ZnO. The peak at 530.83 eV (2) is attributed to the presence of OH bonds. The peaks at higher binding energy of 531.25 eV (3) and 531.64 eV (4) can be ascribed to the specific chemisorbed oxygen, such as –COO bond from acetate group, adsorbed O_2, or adsorbed H_2O [14,15]. In case of Tb doped ZnO nanoparticle [Fig. 3(b)], an additional shoulder at lower binding energy is observed. Here also, signatures of the components of different oxygen species are found. The broad peaks at 530.22 eV and 531.4 eV are likely to be ascribed to the coordination of oxygen in Tb–O–Tb and Tb–O–Zn, respectively [15]. The peaks at higher binding energy positioned at 532.07 eV (3) and 532.31 eV (4) can be ascribed to the chemisorbed oxygen, such as –COO bond from acetate group, adsorbed O_2, or adsorbed H_2O as is observed in case of ZnO nanoparticles. It should be mentioned that the overall peak position of the O1*s* spectra for Tb doped ZnO nanoparticles is shifted to higher energy by 0.85 eV as compared to that for the undoped ZnO nanoparticles, which suggests an incorporation of Tb in the ZnO lattice. Note that a very similar result has been observed in La-doped ZnO nanoparticle sample [14, 15]. The XPS spectra for the core Zn 2$p_{3/2}$ level for these nanoparticles are compared in Fig. 3 (c) and (d). The deconvolution of the spectra indicates that two zinc species exists in ZnO nanoparticles [Fig. 3(c)]. The observed peak (1) at the binding energy of 1022.04 eV is associated to Zn-O-Zn bonding. The other peak (2) with binding energy of 1022.3 eV is believed to be associated with the Zn-OH bonding. The spectrum associated with Zn2$p_{3/2}$ level for Tb doped ZnO nanoparticles [Fig. 3(d)] is also found to be resulting from two types of bonding. However, the overall position of the Zn2$p_{3/2}$ level shows a shift towards higher energies by ~ 0.43 eV for the Tb doped ZnO nanoparticle sample as compared to the undoped ZnO sample, which again suggests the incorporation of Tb in the ZnO lattice [15, 16].

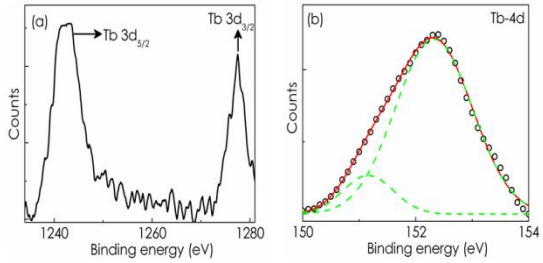

FIGURE 4 (a) Tb-3*d* spectra and (b) Tb-4*d* spectra for Tb doped ZnO nanoparticles for Tb-acetate/Zn-acetate ~ 25%.

Figure 4 (a) and (b) shows the Tb 3*d* and Tb 4*d* spectrum for a Tb doped ZnO nanoparticle sample with Tb-acetate/Zn-acetate ~25%.

Fig. 4 (a) shows the Tb3$d_{5/2}$ and Tb3$d_{3/2}$ peaks present at 1242.4 eV and 1277.53 eV respectively. The Tb3$d_{5/2}$ peak shifts by 0.3 eV from its standard value for the bulk Tb metal.Fig. 4 (b) shows the Tb-4*d* spectrum for Tb doped ZnO nanoparticles with Tb-acetate/Zn-acetate ~25%. The deconvolution of the Tb-4*d* spectrum indicates the presence of two Tb species associated with ZnO lattice. The peak at 151.15 eV (1) is believed to be associated with Tb-O-Tb bonding. The peak at 152.3 eV (2) is attributed to the Tb-O-Zn bonding [16, 17].

CONCLUSION

In conclusion, our study suggests that the Tb accumulates on the surface of ZnO nanoparticles and affects the optical properties of these nanoparticles by influencing the attachment of certain adsorbed groups, which are found to be responsible for the broad band luminescence. Under the atmospheric condition, the major part of the broad band luminescence arises due to the adsorption of certain groups on the surface of the nanoparticles. The density of thes chemical species is found to increase with the Tb mole-fraction, resulting in an increase of broad band luminescence intensity with *x* under the atmospheric condition. The PL and EPR study suggests that for high value of Tb mole-fraction in ZnO nanoparticle, the broad luminescence band results both from the adsorbed chemical species as well as the point defects, which are generated when Tb incorporates in the core of ZnO host lattice. Our XPS results also confirm the presence of several oxygen species adsorbed on the surface. The study thus offers a unique way to control the intensity ratios of both the emission bands in ZnO nanoparticles by adjusting the Tb doping concentration which could be helpful for fabrication of various color LED's. PL studies performed under different environmental conditions (i.e. in the presence of various gases) can be helpful for further application in gas sensors.

ACKNOWLEDGEMENT

The authors acknowledge the support of Prof. S. Dhar, Associate Professor, Departemt of Physics, I.I.T Bombay for fruitful discussion.

REFERENCES

1. Q. Xianga, G. Meng, Y. Zhanga, J. Xua, P. Xu, Q. Pana, W. Yuc,, Sens. Actuators B 143 (2010) 635–640.
2. V. Galstyan, E. Comini, C. Baratto, G. Faglia, G. Sberveglierim, Ceram. Int. 41, 14239–14244 (2015).
3. S. Huang, T. Wang, Q. Xiao, J. Phys. Chem. Solids 76, 51–58 (2015).
4. M. Hjiri, R. Dhahri, K. Omri, L.E. Mir, S.G. Leonardi, N. Donato, G. Neri, Mater. Sci. Semicond. Process. 27, 319–325 (2014).
5. D.R. Patil, L.A. Patil, Talanta,77, 1409–1414 (2009).
6. D. Han, J. Yang, F. Gu, Z. Wang, RSC Adv. http://dx.doi.org/10.1039/C6RA06816B, (2016).
7. O. Singh, R.C. Singh, Mater. Res. Bull. 47 (3) 557–561.
8. C.Y. Tee, G.K. Das, Y. Zhang, T.T.Y. Tan, Pan Stanford Publishing, CRC press, Boca raton, 231–233, (2012).
9. V. Kumar, O.M. Ntwaeaborwa, J. Holsa, D.E. Motaung, H.C. Swart, Opt. Mater. 46 510–516 (2015).
10. A. Sharma, S. Dhar, B. P. Singh, T. Kundu, Solid State Commun. 151, 1885-1888, (2011).
11. W. Göpel, J. Vac. Sci. Technol. 15, 1298 (1978).
12. A. B. Djurišić, W. C. H. Choy, V. A. L. Roy, Y. H. Leung, C. Y. Kwong, K. W. Cheah, T. K. GunduRao, W. K. Chan H. Fei Lui C. Surya, Adv. Funct. Mater. No. 9, 14, 856-864 (2004).
13. D. Daksh, Y. K. Agarwal, Reviews in Nanosci.Nanotechnol. Vol. 5, pp. 1–27, 2016.
14. A. E. Jiménéz-González , J. A. Soto Urueta, R. Suarez-Parra, J. Cryst. Growth 192, 430 (1998).
15. R. Zhang, P. –G. Yin, N. Wang, L. Guo, Solid state Sci., 11, 865 (2009).
16. Y. –M. Hao, S. –Y. Lou, S. –M. Zhou, R. –J. Yuan, G.-Y. Zhu, N. Li, Nano. Scale Res. Lett., 7, 100 (2012).
17. S. M. Liu ,F. Q. Liu, H. Q. Guo, Z. H. Zhang, Z.G. Wang, Phys. Lett. A, 271, 128 (2000).